Title	Radiated seismic energy and energy magnitude
Author	**George L. Choy and John L. Boatwright**, U. S. Geological Survey, Denver, CO 80215; E-mail: choy@usgs.gov
Version	August 2002; editorially adapted and amended July 2012; **DOI: 10.2312/GFZ.NMSOP-2_IS_3.6**

1 Introduction

One of the most fundamental parameters for describing an earthquake is radiated seismic energy. In theory, its computation simply requires an integration of radiated energy flux in velocity-squared seismograms. In practice, energy has historically almost always been estimated with empirical formulas. The empirical approach dominated for two major reasons. First, until the 1980's most seismic data were analog, a format which was not amenable to spectral processing on a routine basis. Second, an accurate estimate of radiated energy requires the analysis of spectral information both above and below the corner frequency of an earthquake, about which energy density is most strongly peaked.

Prior to the worldwide deployment of broadband seismometers, which started in the 1970's, most seismograms were recorded by conventional seismographs with narrowly peaked instrument responses. The difficulties in processing analog data were thus compounded by the limitations in retrieving reliable spectral information over a broad bandwidth. Fortunately, theoretical and technological impediments to the direct computation of radiated energy have been removed. The requisite spectral bandwidth is now recorded digitally by a number of seismograph networks and arrays with broadband capability, and frequency-dependent corrections for source mechanism and wave propagation are better understood now than at the time empirical formulas were first developed.

2 How is radiated seismic energy measured?

2.1 Method

The method described below for estimating the radiated seismic energy of teleseismic earthquakes is based on Boatwright and Choy (1986). Velocity-squared spectra of body waves are corrected for effects arising from source mechanism, depth phases, and propagation through the Earth.

For shallow earthquakes where the source functions of direct and surface-reflected body-wave arrivals may overlap in time, the radiated energy of a *P*-wave group (consisting of *P*, *pP* and *sP*) is related to the energy flux by

$$E_S^P = 4\pi \; <F^P>^2 \left(\frac{R^P}{F^{gP}} \right)^2 \varepsilon_{gP}^* \tag{1}$$

where the P-wave energy flux, ε_{gP}^*, is the integral of the square of the ground velocity, taken over the duration of the body-wave arrival,

$$\varepsilon_{gP}^* = \rho\alpha \int_0^\infty \dot{u}(t)^2 \, dt \tag{2}$$

Here, $\dot{u}$ is velocity, which must be corrected for frequency-dependent attenuation; ρ and α are density and velocity at the receiver, respectively; $<F^P>^2$ is the mean-square radiation-pattern coefficient for *P* waves; R^P is the *P*-wave geometrical spreading factor; F^{gP} is the generalized radiation pattern coefficient for the *P*-wave group defined as

$$\left(F^{gP}\right)^2 = \left(F^P\right)^2 + \left(\hat{PP} \;\; F^{pP}\right)^2 + \frac{2\alpha q}{3\beta}\left(\hat{SP} \;\; F^{sP}\right)^2 \tag{3}$$

where F^i are the radiation-pattern coefficients for $i = P$, pP, and sP; $\hat{PP}$ and $\hat{SP}$ are plane-wave reflection coefficients of *pP* and *sP* at the free surface, respectively, corrected for free-surface amplification; and *q* is 15.6, the ratio of *S*-wave energy to *P*-wave energy (Boatwright and Fletcher, 1984). The correction factors explicitly take into account our knowledge that the earthquake is a double-couple, that measurements of the waveforms are affected by interference from depth phases, and that energy is partitioned between *P* and *S* waves. For teleseismically recorded earthquakes, energy is radiated predominantly in the bandwidth 0.01 to about 5.0 Hz. The wide bandwidth requires a frequency-dependent attenuation correction (Cormier, 1982). The correction is easily realized in the frequency domain by using Parseval's theorem to transform Eq. (2),

$$\varepsilon_{gP}^* = \frac{\rho\alpha}{\pi} \int_0^\infty \dot{u}(\omega)^2 e^{\omega t_\alpha^*} \, d\omega \tag{4}$$

where t_α^* is proportional to the integral over ray path of the imaginary part of complex slowness in an anelastic Earth. An appropriate operator, valid over the requisite broad bandwidth, is described by Choy and Cormier (1986) and shown in Figure 1. The t_α^* of the *P*-wave operator ranges from 1.0 s at 0.1 Hz to 0.5 s at 2.0 Hz.

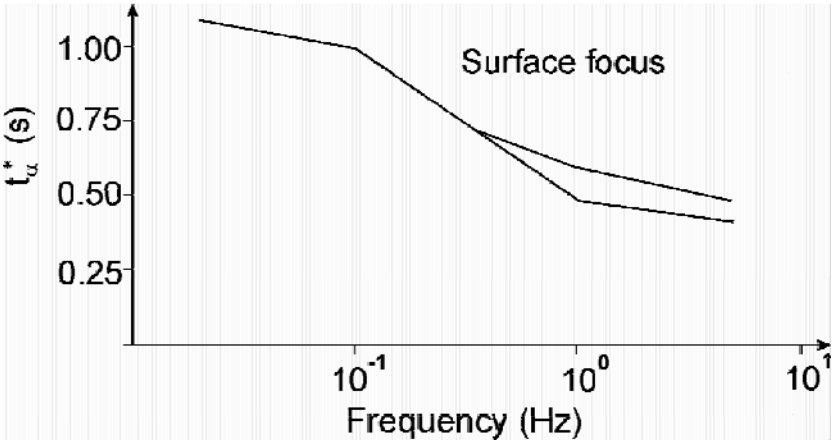

Figure 1 Teleseismic t^*_α derived by Choy and Cormier (1986) plotted as a function of frequency for a surface-focus source and a surface receiver at a distance of 60°. The split in the curve at frequencies higher than 0.3 Hz indicates the variation in regional t^*_α expected for different receiver sites. In practice the mean of the two curves is used for the attenuation correction.

The numerical integration of Eq. (4) is limited to either the frequency at which signal falls below the noise level (typically at frequencies greater than 2.0-3.0 Hz) or to the Nyquist frequency. If this limiting or cutoff frequency, ω_c, is greater than the corner frequency, the remainder of the velocity spectrum is approximated by a curve that falls off by ω^{-1}. In practice, therefore, Eq. (4) consists of a numerical integral, *N*, truncated at ω_c, and a residual integral, *R*, which approximates the remainder of the integral out to infinite frequency,

$$\varepsilon^*_{gP} = \rho\alpha N + \rho\alpha R \tag{5}$$

where, as shown in Boatwright and Choy (1986),

$$R = \frac{\omega_c}{\pi}\left[\dot{u}_c(\omega_c)\right]^2 \tag{6}$$

in which $\dot{u}_c$ is the attenuation-corrected value of velocity at ω_c.

Although teleseismic *SH*- and *SV*-wave groups from shallow earthquakes can be analyzed through a straightforward extension of Eq. (1) as described in Boatwright and Choy (1986), shear waves suffer substantially more attenuation in propagation through the Earth than the *P* waves. The loss of seismic signal due to shear attenuation usually precludes retrieving useful spectral information for frequencies higher than about 0.2-0.3 Hz for all but the largest earthquakes. Thus, for the routine estimation of energy, it is more practical and more accurate to use only the *P*-wave group (Eqs. (1) and (4)). The formula for computing the total radiated energy when using the *P*-wave group alone is

$$E_s = (1+q)\,E_s^P\,. \tag{7}$$

2.2 Data

Data used in the direct measurement of energy must satisfy three requirements. First, the implementation of Eq. (4) requires that the velocity data contain spectral information about, above and below the corner frequency of an earthquake. Because the corner frequency can vary from earthquake to earthquake depending on source size and rupture complexity, the bandwidth of the data must be sufficiently wide so that it will always cover the requisite range of frequencies above and below the corner frequency. For body waves from teleseismically recorded earthquakes, a spectral response that is flat to ground velocity between 0.01 Hz through 5.0 Hz is usually sufficient. The second requirement is that the duration of the time window extracted from a seismogram should correspond to the time interval over which the fault is dynamically rupturing. As shown by the examples in Figure 2, when broadband data are used, delimiting the time window is generally unequivocal regardless of the complexity of rupture or the size of the earthquake. The initial arrival of energy is obviously identified with the onset of the direct *P* wave. The radiation of energy becomes negligible when the amplitude of the velocity-squared signal decays to the level of the coda noise. The final requirement is that we use waveforms that are not complicated by triplications, diffractions or significant secondary phase arrivals. This restricts the usable distance range to stations within approximately 30°-90° of the epicenter. In addition, waveforms should not be used if the source duration of the *P*-wave group overlaps a significant secondary phase arrival. For example, this may occur when a very large earthquake generates a *P*-wave group with a duration of such length that it does not decay before the arrival of the *PP*-wave group.

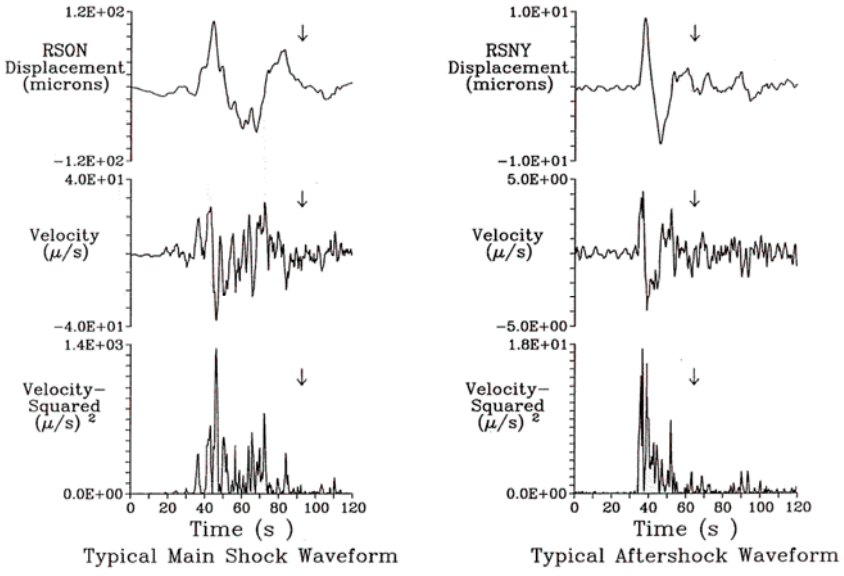

Figure 2 (Left) Broadband displacement, velocity, and velocity-squared records for the large (Ms = 7.8, Me = 7.5, Mw = 7.7) Chilean earthquake of 3 March 1985. Rupture complexity, in the form of a tiny precursor and a number of sub-events, is typical for large earthquakes. **(Right)** Broadband displacement, velocity and velocity-squared records for an aftershock (mb = 5.9, Me = 6.2, Mw = 6.6) to the Chilean earthquake that occurred 17 March 1985. The waveforms are less complex than those of the main shock. Despite the differences in rupture complexity, duration and amplitude, the time window over which energy arrives is unequivocal. In each part of the figure the arrows indicate when the velocity-squared amplitude has decreased to the level of the coda noise.

3 Development of an energy magnitude, Me

In the Gutenberg-Richter formulation, an energy is constrained once magnitude is known through log E_S = a + b M where *a* and *b* are constants. For surface-wave magnitude, Ms, the Gutenberg-Richter formula takes the form

$$\log E_S = 4.8 + 1.5\ Ms \tag{8}$$

where E_S is in units of Joules (J). In the normal usage of Eq. (8), an energy is derived after an Ms is computed. However, it is now recognized that for very large earthquakes or very deep earthquakes, the single frequency used to compute Ms is not necessarily representative of the dimensions of the earthquake and, therefore, might not be representative of the radiated energy. Since radiated energy can now be computed directly, it is an independent parameter from which a unique magnitude can be defined. In Figure 3, the radiated energies for a set of 378 global shallow earthquakes from Choy and Boatwright (1995) are plotted against their magnitudes, Ms. The Gutenberg-Richter relationship is plotted as a dashed line in Figure 3. Assuming a b-value of 1.5, the least-squares regression fit between the actual energies and magnitude is

$$\log E_S = 4.4 + 1.5\ Ms \tag{9}$$

which is plotted as the solid line in Figure 3. The *a*-value of 4.4 indicates that on average the original Gutenberg-Richter formula overestimates the radiated energy by a factor of two. To define energy magnitude, Me, we replace Ms with Me in Eq. (9)

$$\log E_S = 4.4 + 1.5\ Me \tag{10}$$

or

$$Me = (\log E_S - 4.4)/1.5. \tag{11}$$

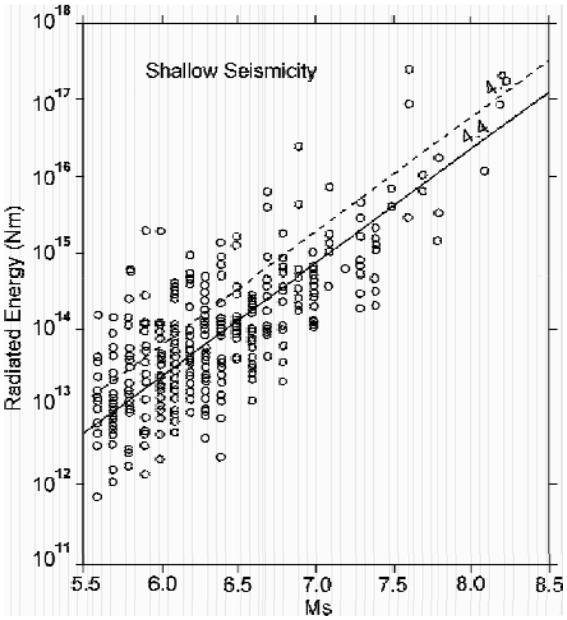

Figure 3 Radiated energy (E_S) of global data as a function of surface-wave magnitude (Ms). The energy predicted by the Gutenberg-Richter formula, log E_S = 4.8 + 1.5 Ms (in units of Newton-meters), is shown by the dashed line. From a least-squares regression, the best-fitting line with the slope of 1.5 is log E_S= 4.4 + 1.5 Ms (according to Choy and Boatwright, 1995).

The usage of Eq. (11) is conceptually antithetical to that of Eq. (8). In Eq. (11) magnitude is derived explicitly from energy, whereas in Eq. (8) energy is dependent on the value of magnitude.

4 The relationship of radiated energy to moment and apparent stress

The energy and moment for a particular earthquake are related by apparent stress, σ_{app} (see Equation (59) in IS 3.1),

$$\sigma_{app} = \mu \, E_S / M_0 \tag{12}$$

where μ is the average rigidity at the source. When radiated energy, E_S, is plotted against seismic moment, M_0, for global shallow earthquakes (Figure 4), the best fit by least-squares regression of E_S on M_0 (solid line) yields

$$E_S = 1.6 \cdot 10^{-5} M_0. \tag{13}$$

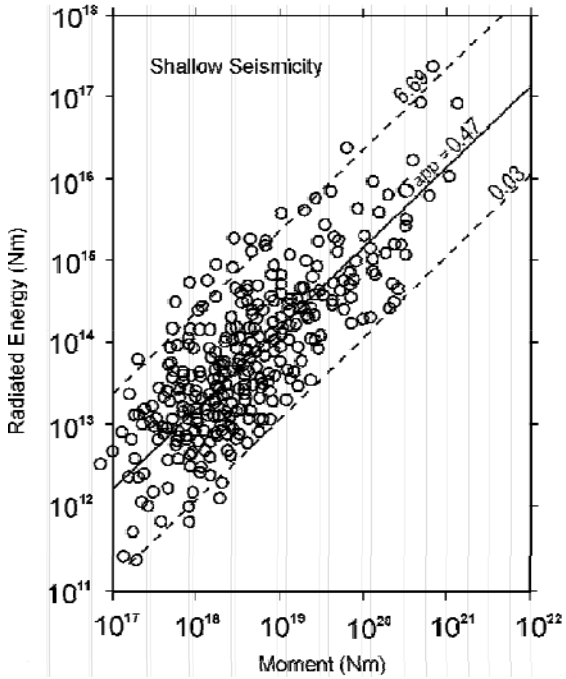

Figure 4 Radiated energy, E_S, of 394 shallow-focus earthquakes as a function of seismic moment, M_0 . The slope of the least-squares log-normal regression (solid line) yields a global average apparent stress $\overline{\sigma}_{app}$ of about 0.5 MPa assuming a source rigidity of $0.3 \cdot 10^5$ MPa. The 95% spread (or width of distribution) about the regression line is indicated by the dashed lines (according to Choy and Boatwright, 1995).

Assuming an average rigidity for shallow earthquakes of $0.3 \cdot 10^5$ MPa, the slope of the regression line yields a worldwide average apparent stress, $\overline{\sigma}_{app}$ of about 0.47 MPa. The spread about the regression line is very large. In terms of apparent stress it is between 0.03 to 6.69 MPa. Empirical formulas, like those employing M_0 or Ms, ignore the spread and, thus,

would be poor predictors of energy. Viewing the spread of E_S-M_0 values about the regression line in terms of apparent stress, rather than random scatter, may provide significant insight into the physics of earthquake occurrence. For example, the release of energy and apparent stress could vary systematically as a function of faulting type, lithospheric strength and tectonic region (Choy and Boatwright,1995). As more statistics on the release of energy are accumulated, spatial and temporal variations in energy release and apparent stress might also be identified.

5 The relationship of Me to Mw

Although Me and Mw are magnitudes that describe the size of an earthquake, they are not equivalent. Me, being derived from velocity power spectra, is a measure of the radiated energy in form of seismic waves and thus of the seismic potential for damage to anthropogenic structures. Mw, being derived from the low-frequency asymptote of displacement spectra, is physically related to the final static displacement of an earthquake. Because they measure different physical properties of an earthquake, there is no *a priori* reason that they should be numerically equal for any given seismic event. The usual definition of Mw is:

$$Mw = 2/3 \log M_0 - 6.0 \qquad \text{(with } M_0 \text{ in Nm).} \qquad (14)$$

The condition under which Me is equal to Mw, found by equating Eq. (11) and Eq. (14), is $E_S/M_0 \sim 2.2 \cdot 10^{-5}$. From Eq. (12) this ratio is equivalent to $\sigma_{app} \sim 2.2 \cdot 10^{-5} \mu$. For shallow earthquakes, where $\mu \sim 0.3\text{-}0.6 \times 10^5$ MPa, this condition implies that Me and Mw will be coincident only for earthquakes with apparent stresses in the range 0.66-1.32 MPa. As seen in Figure 4, this range is but a tiny fraction of the spread of apparent stresses found for earthquakes. Therefore, the energy magnitude, Me, is an essential complement to moment magnitude, Mw, for describing the size of an earthquake. How different these two magnitudes may be is illustrated in Table 1. Two earthquakes occurred in Chile within months of each other and their epicenters were less than 1º apart. Although their Mw's and Ms's were similar, their mb's and Me's differed by 1 to 1.4 magnitude units! Table 1 describes the macroseismic effects from the two earthquakes. The event with larger Me caused significantly greater damage!

Table 1 (Reprinted from Choy et al., 2001.)

Date	LAT (°)	LON (E)	Depth (km)	Me	Mw	mb	Ms	$sigma_a$ (bars)	Faulting Type
6 JUL 1997 (1)	-30.06	-71.87	23.0	**6.1**	**6.9**	**5.8**	**6.5**	1	**interplate-thrust**
15 OCT 1997 (2)	-30.93	-71.22	58.0	**7.5**	**7.1**	**6.8**	**6.8**	44	**intraslab-normal**

(1) Felt (III) at Coquimbo, La Serena, Ovalle and Vicuna.

(2) Five people killed at Pueblo Nuevo, one person killed at Coquimbo, one person killed at La Chimba and another died of a heart attack at Punitaqui. More than 300 people injured, 5,000 houses destroyed, 5,700 houses severely damaged, another 10,000 houses slightly damaged, numerous power and telephone outages, landslides and rockslides in the epicentral region. Some damage (VII) at La Serena and (VI) at Ovalle. Felt (VI) at Alto del Carmen and Illapel; (V) at Copiapo, Huasco, San Antonio, Santiago and Vallenar; (IV) at Caldera, Chanaral, Rancagua and Tierra Amarilla; (III) at Talca; (II) at Concepcion and Taltal. Felt as far south as Valdivia. Felt (V) in Mendoza and San Juan Provinces, Argentina. Felt in Buenos Aires, Catamarca, Cordoba, Distrito Federal and La Rioja Provinces, Argentina. Also felt in parts of Bolivia and Peru.

6 Regional estimates of radiated seismic energy

Radiated energy from local and regional records can be computed in a fashion analogous to the teleseismic approach if suitable attenuation corrections, local site and receiver effects, and hypocentral information are available or can be derived. Boatwright and Fletcher (1984) demonstrated that integrated ground velocity from S waves could be used to estimate radiated energy in either the time or frequency domain by,

$$E_s = 4\pi C^2 r^2 \rho_r \beta_r \int_0^\infty \dot{u}_c(t)^2 dt \tag{15}$$

$$= 4\pi C^2 r^2 \rho_r \beta_r \int_0^\infty \dot{u}_c(\omega)^2 \, d\omega \tag{16}$$

where the ground velocity has been corrected for anelastic attenuation, C is a correction for radiation pattern coefficient and free-surface amplification, r is the source-receiver distance, and ρ_r and β_r are density and S-wave velocity at the receiver. The attenuation correction is usually of the type $exp(\omega r/\beta Q)$, where Q is the whole-path attenuation. Similarly, Kanamori et al. (1993) use a time-domain method to estimate the S-wave energy radiated by large earthquakes in southern California,

$$E_\beta = 4\pi r^2 C_f^{-2} \left[r_0 q(r_0)/rq(r) \right]^2 \rho_0 \beta_0 \int_0^\infty \dot{u}^2(t) dt \tag{3.66}$$

where ρ_0 and β_0 are hypocentral density and S-wave velocity, C_f is the free-surface amplification factor, r is the source-receiver distance estimated from the epicentral distance Δ and a reference depth h of 8 km (such that $r^2=\Delta^2+h^2$). Attenuation is described by $q(r) = cr^{-n} \exp(-kr)$, which is the Richter (1935) attenuation curve as corrected by Jennings and Kanamori (1983). For southern California earthquakes, c=0.49710, n=1.0322, and k=0.0035 km^{-1}.

7 Conclusions

Energy gives a physically different measure of earthquake size than moment. Energy is derived from the velocity power spectra, while moment is derived from the low-frequency asymptote of the displacement spectra. Thus, energy is a better measure of the severity of shaking and thus of the seismic potential for damage, while moment, being related to the final static displacement, is more related to the long-term tectonic effects of the earthquake process. Systematic variations in the release of energy and apparent stress as a function of faulting type and tectonic setting can now be identified that were previously undetectable because of the lack of reliable energy estimates. An energy magnitude, Me, derived from an explicit computation of energy, can complement Mw and Ms in evaluating seismic and tsunamigenic potential.

Recommended overview readings

Bormann and Di Giacomo (2011)
Di Giacomo and Bormann (2011)
Choy and Boatwright (1995)
Choy et al. (2006)
Choy (2012)

References

Bormann, P., and D. Di Giacomo (2011). The moment magnitude M_w and the energy magnitude M_e: common roots and differences. *J. Seismology*, **15**, 411-427; doi: 10.1007/s10950-010-9219-2.

Boatwright, J., and Fletcher, J. B. (1984) The partition of radiated energy between P and S waves, *Bull. Seism. Soc. Am.*, **74**, 361-376.

Boatwright, J., and Choy, G. (1986). Teleseismic estimates of the energy radiated by shallow earthquakes. *J. Geophys. Res.*, **91**, B2, 2095-2112.

Choy, G. L. (2012). IS 3.5:Stress conditions inferable from modern magnitudes: development of a model of fault maturity. In: Bormann, P. (Ed.) (2012). *New Manual of Seismological Observatory Practice (NMSOP-2)*, *IASPEI*, GFZ German Research Centre for Geosciences, Potsdam, 10 pp.; DOI: 10.2312/GFZ.NMSOP-2_IS_3.5.

Choy, G. L., and Cormier, V. F. (1986). Direct measurement of the mantle attenuation operator from broadband P and S Waveforms. *J. Geophys. Res.*, **91**, 7326-7342

Choy, G. L., and Boatwright, J. L. (1995). Global patterns of readiated seismic energy and apparent stress. *J. Geophys. Res.*, **100**, B9, 18,205-18,228.

Choy, G. L., and Kirby, S. H. (2004). Apparent stress, fault maturity and seismic hazard for normal-fault earthquakes at subduction zones, *Geophys. J. Int.*, **159**, 991-1012.

Choy, G. L., McGarr, A., Kirby, S. H., and Boatwirght, J. (2006). An overview of the global variability in radiated energy and apparent stress; in: Abercrombie R. , McGarr, A., and Kanamori, H. (eds): Radiated energy and the physics of earthquake faulting, *AGU Geophys. Monogr. Ser.* **170**, 43-57.

Cormier, V. F. (1982). The effect of attenuation on seismic body waves. *Bull. Seism. Soc. Am.*, **72**, 1, 169-200.

Di Giacomo, D., and Bormann, P. (2011). Earthquake energy. In: Harsh Gupta (ed.). *Encyclopedia of Solid Earth Geophysics,* Springer, 233-236; doi: 10.1007/978-90-481-8702-7.

Jennings, P. C., and Kanamori, H. (1983). Effect of distance on local magnitudes found from strong motion records. *Bull. Seism. Soc. Am.*, **73**, 265-280.

Kanamori, H., Mori, J., Hauksson, E., Heaton, Th. H., Hutton, L. K., and Jones, L. M. (1993). Determination of earthquake energy release and M_L using TERRASCOPE. *Bull. Seism. Soc. Am.*, **83**, 2, 330-346.

Richter, C. F. (1935). An instrumental earthquake magnitude scale. *Bull. Seism. Soc. Am.*, **25**, 1-32.